Journal of Environmental Radioactivity 138 (2014) 264–275

Contents lists available at ScienceDirect

Journal of Environmental Radioactivity

journal homepage: www.elsevier.com/locate/jenvrad

Five-minute resolved spatial distribution of radiocesium in sea sediment derived from the Fukushima Dai-ichi Nuclear Power Plant

Daisuke Ambe [a, *], Hideki Kaeriyama [a], Yuya Shigenobu [a], Ken Fujimoto [a], Tsuneo Ono [a], Hideki Sawada [b, 1], Hajime Saito [b, 2], Shizuho Miki [a], Takashi Setou [a], Takami Morita [c, 2], Tomowo Watanabe [a]

[a] National Research Institute of Fisheries Science, Fisheries Research Agency, 2-12-4, Fukuura, Kanazawa-ward, Yokohama, Kanagawa 236-8648, Japan
[b] National Research Institute of Fisheries Engineering, Fisheries Research Agency, 7620-7, Hasaki, Kamisu, Ibaraki 314-0408, Japan
[c] Fisheries Agency, 1-2-1, Kasumigaseki, Chiyoda-ward, Tokyo 100-8907, Japan

ARTICLE INFO

Article history:
Received 21 January 2014
Received in revised form
3 September 2014
Accepted 14 September 2014
Available online 30 September 2014

Keywords:
Nuclear accident
Sea sediment
Cs-134 and Cs-137
Grain size
Organic matter
Bottom seawater

ABSTRACT

The spatial distributions of radiocesium concentration in sea sediment to a core depth of 14 cm were investigated in the offshore region from the Fukushima Prefecture to the northern part of the Ibaraki Prefecture in February and July 2012, at a spatial resolution of 5 min of latitude and longitude. The concentrations in the area south of the Fukushima Dai-ichi Nuclear Power Plant (FDNPP) were generally higher than those in the area north of it. In the southern area, a band of especially high concentration with a width about 20 km was present in the region shallower than 100 m, and a narrow minimal concentration band was found along the 200-m isobaths. In more than half of all cases, the vertical core profiles of radiocesium concentration generally showed an exponential decreasing trend with depth. However, in the area north of the FDNPP, where the radiocesium concentrations tended to be very low, radiocesium concentrations that had similar or larger magnitude compared with those of the most-surface layer were often found in deeper layers. Relatively good correlations were found between radiocesium concentrations and grain sizes of the most-surface sediment. The vertical profile of radiocesium concentration also had a relationship with grain size. In other case, the radiocesium concentration in the sediment seems to have had a dependence on the radiocesium concentration in bottom seawater, suggesting that the quantity of radiocesium supplied and the grain size were major factors determining the spatial distribution pattern of the radiocesium concentration after the FDNPP accident.

1. Introduction

Following the Great Earthquake and ensuing tsunami that occurred east of Japan on March 11 2011, the cooling functions for the reactors of the Fukushima Dai-ichi Nuclear Power Plant (FDNPP) of Tokyo Electric Power Co., Inc. (TEPCO) were stopped. In the early stage of this accident, the emergency measure for cooling reactors was taken by using fresh water and seawater. Subsequently, a large amount of anthropogenic radionuclides was directly discharged into the sea environment through leakage of this wastewater (Buesseler et al., 2011; Tsumune et al., 2012). The main radionuclides discharged were ^{131}I, ^{134}Cs, and ^{137}Cs, as reported by TEPCO (2012). Because ^{131}I has a short half-life period of about 8.02 d, it cannot be detected at present. However, the two isotopes of radiocesium, ^{134}Cs and ^{137}Cs, which have a much longer half-life (2.06 y and 30.17 y, respectively) than ^{131}I, remain in the environment and will be present for a substantial amount of time.

Cesium, one of the alkali metals, is readily soluble in seawater, hence seawater contains 2 nM of natural stable cesium everywhere in the ocean. Cesium has a highly adsorptive nature on mineral substances, with a distribution coefficient between marine sediment and sea water of 300–4000 L/kg-dry (IAEA, 2004). Cesium is also taken in by organisms and their subsequent organic sediments on the seabed (e.g. Honda et al., 2013). It is thus considered that the FDNPP-derived radiocesium at the accident was transported and diffused in the ocean mainly as both dissolved ion and adsorbate on suspended particles. Several numerical simulation studies of the

* Corresponding author. Tel.: +81 45 788 7654.
E-mail address: ambe@affrc.go.jp (D. Ambe).
[1] Present address: Maizuru Fisheries Research Station, Field Science Education and Research Center, Kyoto Univ., Nagahama, Maizuru, Kyoto 625-0086, Japan.
[2] Present address: Head Office of Fisheries Research Agency, Queen's Tower B 15F, 2-3-2, Minatomirai, Nishi-ward, Yokohama, Kanagawa 220-6115, Japan.

http://dx.doi.org/10.1016/j.jenvrad.2014.09.007

movement of the dissolved radiocesium (e.g., Masumoto et al., 2012; Tsumune et al., 2012) demonstrated that the water mass polluted by radiocesium was transported southward from the FDNPP and finally diffused eastward far from the coast by the Kuroshio and Kuroshio Extention. As a result, based on in situ surveys (e.g., Aoyama et al., 2012; Buesseler et al., 2011; Oikawa et al., 2013), the radiocesium concentration in seawater on the Pacific side of east Japan decreased quickly for several months after the discharge.

Nevertheless, relatively high concentrations of radiocesium have been detected continuously in sea bottom sediment off the eastern coast of Japan since the FDNPP accident (Kusakabe et al., 2013; Otosaka and Kobayashi, 2013; Thornton et al., 2013). The coastal area of eastern Japan is a good fishing ground and an important nursery ground for demersal fishes such as flounder (e.g., Wada et al., 2012). Additionally, Wada et al. (2013) reported that the radiocesium concentrations in some demersal fish species, those that feed mainly on benthic prey, were often higher than and showed slower decrease trends than those of pelagic fish species off Fukushima Prefecture. Because radiocesium bound to sedimentary organic matter has been shown to be dissoluble (e.g. Otosaka and Kobayashi, 2013), some of the radiocesium in the sea bottom sediment could possibly be incorporated into the benthic ecosystem. Thus, it is extraordinarily important to primarily understand the present distribution and/or dynamics of radiocesium in the sea floor sediments to evaluate the potential impact on benthic marine ecosystems and demersal fishes offshore from the prefectures near the FDNPP.

To date, a few studies of the distribution of radiocesium derived from the FDNPP accident on the sea bed have been completed. Otosaka and Kobayashi (2013) reported features of the radiocesium distribution by collecting sediments at nine stations off Ibaraki

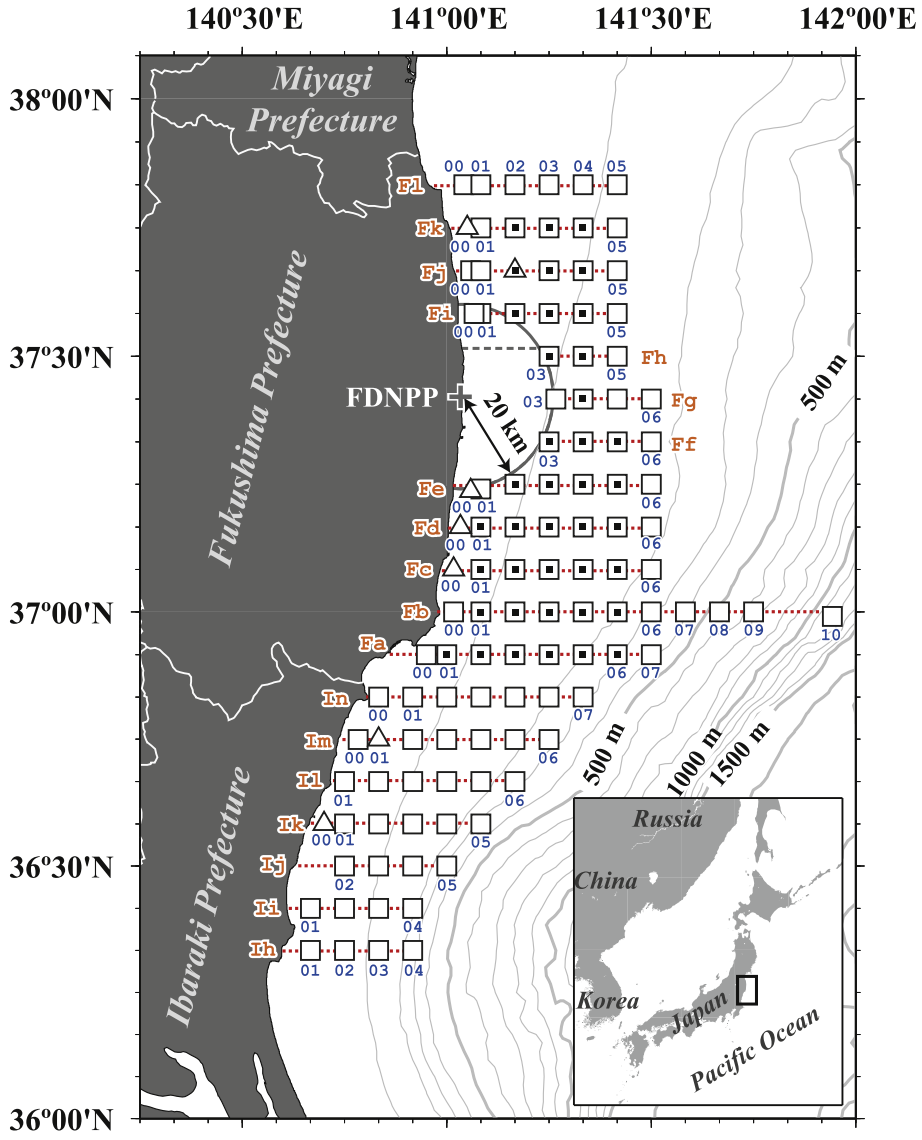

Fig. 1. Survey points for radiocesium concentration in seabed sediment. Dots indicate survey locations with a G.S.-type core sampler in February 2012. In July 2012, sediments were sampled with a G.S.-type core sampler (squares) and a Smith–McIntyre sampler (triangles). The station names corresponding to sampling locations are given in Table S1 by a combination of the latitudinal representation name (red letters) and eastward sequence number on each line of latitude (blue letters). Contour lines indicate water depth at an interval of 100 m. During the survey period in February, a caution zone had been established within a 20-km radius (solid arc) of the Fukushima Dai-ichi Nuclear Power Plant (FDNPP; indicated by cross), and in July, the northern part of the caution zone (border is shown by dotted black line) was neutralized. (For interpretation of the references to color in this figure legend, the reader is referred to the web version of this article.)

Prefecture. Kusakabe et al. (2013) compiled surface-sediment radiocesium concentration data from samples collected at 30 stations in the wide area from the Ibaraki to the Miyagi Prefecture. Although these reports show the distribution of sea bottom radiocesium with a spatial resolution of around several tens of kilometers, detailed spatial features remain unclear. Thornton et al. (2013) directly towed a gamma ray spectrometer to obtain the radiocesium distribution in bottom sediments with a resolution of several tens of meters; however, their method can neither reveal the vertical profile of the radiocesium concentration in the sediment, nor cover the two-dimensional distribution of radiocesium for wide area. In the present study, the distribution of radiocesium in sea sediment was investigated at a 5′ × 5′ grid scale to comprehend the fine-scale features of the sea-bottom radiocesium distribution along prefectures near the FDNPP. Here, we report that the distribution of radiocesium concentration in sea sediment depends on the sediment grain-size of the sediment, and the radiocesium concentration in bottom seawater.

2. Materials and methods

Field surveys of sea sediment were conducted during two periods, from February 1–4 and from July 11–16, 2012, by the R/V *Soyo Maru* (Fisheries Research Agency, Japan). In the former investigation (hereafter called SY1202), sediment samples were collected at 40 locations off Fukushima which were arrayed at every 5 min of latitude and longitude (dots in Fig. 1). In the latter investigation (hereafter SY1207), sediment samples were collected at 113 locations (open squares and triangles in Fig. 1). Of the 113 locations, 95 were arrayed with the same spatial resolution used for SY1202, and 18 supplementary locations were set near the coast at a depth of about 25 m or on a 20 km radius from the FDNPP on each parallel of latitude; admittance in the survey period of SY1202 was limited to outside of the 20-km radius from the FDNPP, but the northern part of that radius was admitted before the SY1207 survey. The station names corresponding to sampling locations were established by a combination of the latitudinal representation name (red letters in Fig. 1) and the eastward sequence number on each line of latitude (blue letters in Fig. 1). In both surveys, undisturbed 14-cm deep sea-sediment columns were collected mainly by using a triple-tube core sampler with a lid system (No. 5174, Rigo Co., LTD, Tokyo, Japan). The sampled sediment columns were immediately pushed out from the tubes and divided into six layers, 0–1, 1–2, 2–4, 4–6, 6–10, and 10–14 cm. In this process, the sediments of the most-surface layer (0–1 cm) were sampled with small amount of seawater which was immediately above the sediment to obtain full sediment sample. In addition, the outer part of sediment core samples deeper than 0–1 cm was cut off to avoid the vertical data contamination. And then, the obtained samples were refrigerated on shipboard. The core sampler could not be used at some locations in SY1207 because of rigid sediment material, so sediments were collected with a Smith-McIntyre sampler (No. 5144-B, Rigo Co., LTD, Tokyo, Japan) and the surface layer (0–1 cm) was subsampled.

In the laboratory, the sediment samples were dried at 60 °C for 7 d. Then, specific gamma rays of ^{134}Cs (604 and 795 keV) and ^{137}Cs (661 keV) from those samples were measured for 7200 s using a Ge semiconductor detector (Seiko EG & G, ORTEC, Tennessee, USA). The counting efficiency of the Ge semiconductor detector was calibrated using volume standard sources (MX033SPSV, the Japan Radioisotope Association (JRA), Tokyo, Japan). Coincidence summing effects of ^{134}Cs were corrected with ^{134}Cs standard solutions (CZ005, JRA, Tokyo, Japan). From the measured results, concentrations of radiocesium were calculated as Bq/kg-dry. The concentrations of radiocesium were decay corrected to the date and time of the sampling. The concentration of three times of the standard deviation from counting statistics was defined as the detection limit concentration. The detection limits of the two isotopes of radiocesium in the sea-bottom sediment analyzed in this study were both approximately in the range from 0.63 to 3.0 Bq/kg-dry.

In addition to radiocesium concentration, two more analyses were conducted for the most-surface sediment at each station. The median grain size was calculated from particle size histograms obtained using a laser diffraction analyzer (SALD-3100, Shimadzu, Kyoto, Japan), and the organic matter content of the sediments was determined following the Japan Industrial Standards method (JIS A 1226). The latter analysis was applied only to samples from the SY1207 survey. For this analysis, 3–7 g of sediment was dried at 110 °C for 24 h. Then, the dried sediment was heated at 750 °C for 1 h in a muffle furnace. The organic matter content was determined by the loss of sediment mass.

3. Results

Fig. 2 shows the distributions of ^{134}Cs and ^{137}Cs concentrations in each sea sediment layer obtained in SY1202. In the most-surface sediment layer, the ^{137}Cs concentration varied largely from 18.0 Bq/kg-dry to 1.12 kBq/kg-dry (Fig. 2g). The geometric mean of these samples was 120 Bq/kg-dry and the geometric standard deviation was 0.41. The concentrations in this layer tended to be higher in the area south of the FDNPP (<37°25′N; geometric mean of 145 Bq/kg-dry, geometric standard deviation of 0.21) than in the area north of it (>37°25′N; geometric mean of 75.9 Bq/kg-dry, geometric standard deviation of 0.30). In the southern area, particularly high concentrations of more than 300 Bq/kg-dry were found in the nearshore region shallower than about 100 m. In the off-shore region, the concentration generally decreased toward the east but increased again at some of the easternmost survey points (Stations Fb05, Fc05, and Fd05). On the other hand, in the northern area, relatively low concentrations of less than 30.0 Bq/kg-dry were often found in the region shallower than 100 m. Features similar to those of the horizontal pattern of the most-surface sediment layer were also observed in the lower sediment layers, although these concentrations generally decreased with sediment depth. Cesium-134, whose half-life is 2.06 y, was also detected at all survey positions in the upper four layers, indicating that the radioactive contamination reached a depth of from 4 to 6 cm by 11 months after the FDNPP accident.

Fig. 3 shows the distributions of ^{134}Cs and ^{137}Cs concentrations obtained in SY1207. The magnitudes of ^{137}Cs concentrations in SY1207 were similar to those of SY1202; the ^{137}Cs concentrations in the most-surface sediment layer ranged from 8.8 Bq/kg-dry to 1.24 kBq/kg-dry (Fig. 3g). The geometric mean and geometric standard deviation of these samples were 100 Bq/kg-dry and 0.43. The pattern of the horizontal distribution of ^{137}Cs concentrations in SY1207 was also similar to that of SY1202 off Fukushima Prefecture. In addition to the spatial patterns revealed by SY1202, the SY1207 survey revealed several additional features of the horizontal ^{137}Cs distribution. For example, in the region north of the FDNPP (>37°25′N), although low concentrations were often found in the region shallower than 100 m, relatively high concentrations of more than 300 Bq/kg-dry were found at some locations in the most coastal survey area (Stations Fj00 and Fk00). However, the opposite pattern was obtained in the region south of the FDNPP. Specifically, while a band of high concentrations exceeding 200 Bq/kg-dry with an east–west width of about 15–20 km (longitudinal 5-min grid interval of about 7.4 km at 37°N) was found, relatively lower concentrations of about 20–150 Bq/kg-dry occurred at some locations in the most coastal survey area (Stations Ii01, Ik00, Il01, Im00, Fa00, and Fe00). The concentrations also generally decreased eastward

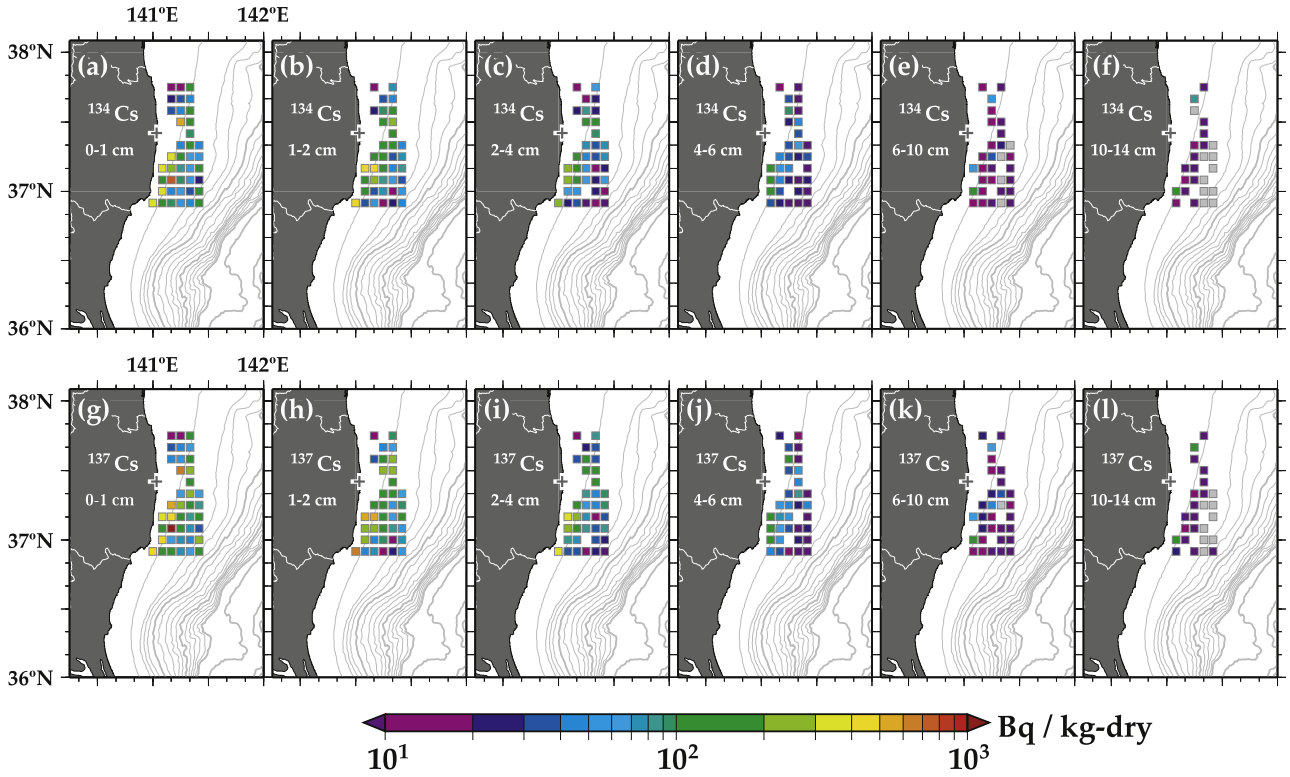

Fig. 2. Spatial distributions of ^{134}Cs (a–f) and ^{137}Cs (g–l) concentrations in sediment in February 2012. The respective nuclide and layer are indicated at left side of each panel. The color scale for the tiles shows the concentration value. Gray tiles mean that radiocesium was not detected (concentration was less than the lower limit of detection). Blank tiles mean missing data associated with the absence of sample. Thin and thick contour lines indicate water depth at every 100 and 500 m, respectively. Cross indicates the location of the FDNPP.

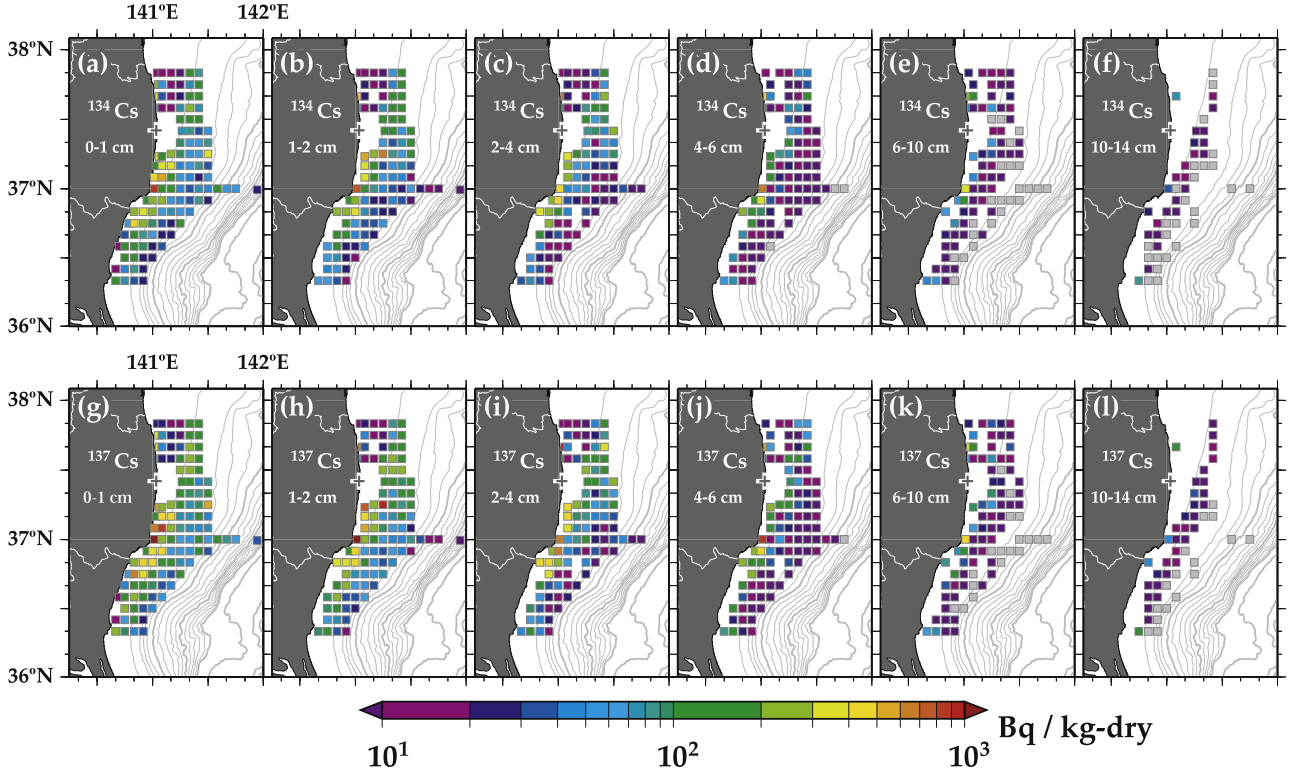

Fig. 3. Same as Fig. 2 but for July 2012.

from the high concentration band. However, a narrow minimal concentration band (at least less than 15 km in width) of 30–60 Bq/kg-dry existed around the 200-m isobaths about 20–30 km east from the high concentration band (Stations Ij04, Ik04, Il05, Im05, Fa05, Fb04, and Fc05); for instance, the ^{137}Cs concentration values at Stations Fb02–06 were 150 ± 4, 60.2 ± 2.5, 50.0 ± 2.1, and 109 ± 5 Bq/kg-dry, respectively (see also Table S1 for the other latitude lines). The ^{134}Cs and ^{137}Cs concentrations at the eastern-most survey point off of the southern part of Fukushima (Station Fb10) were 23 and 37 Bq/kg-dry, respectively (Fig. 3a, b).

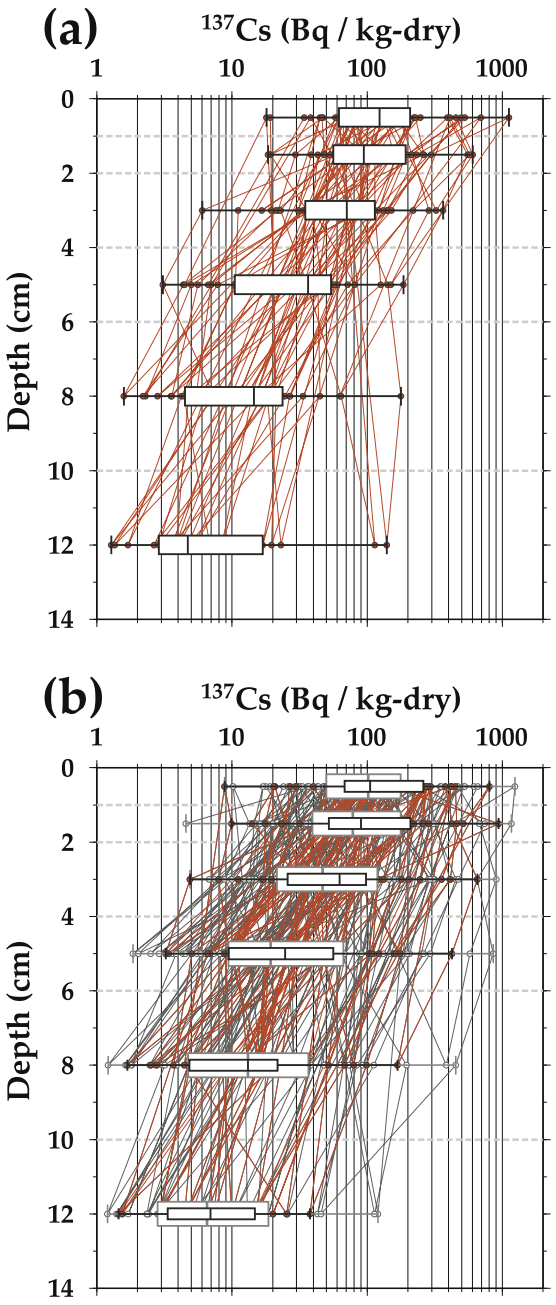

Fig. 4. The acquired vertical profiles (thin lines with circles) of ^{137}Cs concentration in February (a) and July (b). The box and whisker plot shows the minimum value, the 25th, the 50th, and the 75th percentiles, and the maximum value, respectively, in each layer. For descriptive purposes, the red profiles and the black box and whisker plots indicate the common survey points in February and July. (For interpretation of the references to color in this figure legend, the reader is referred to the web version of this article.)

Fig. 4 shows all the acquired vertical profiles of the ^{137}Cs concentrations in the sea sediment of SY1202 and SY1207. Although the concentration values varied largely over a range of more than two orders in many layers of both surveys, the values from the 25th to 75th percentile were within one order range. The median value concentrations of each layer generally decreased exponentially with depth, and the magnitudes of these values were similar in both surveys. The median values in the 0–1, 1–2, 2–4, 4–6, 6–10, and 10–14 cm layers were 124, 94.3, 70.5, 36.6, 14.5, and 4.70 Bq/kg-dry in SY1202 and 105, 90.1, 62.5, 24.7, 13.1, and 6.94 Bq/kg-dry at the same area in SY1207, respectively. However, concentrations larger than those in the most-surface sediment sometimes appeared in lower layers at some survey points; such cases occurred at 45% and 42% of all survey positions in SY1202 and SY1207, respectively.

Fig. 5 shows the horizontal distribution of the median grain-size values of the most-surface sediment in SY1207. The distribution in SY1202 is not shown here because the distribution features in SY1202 were mostly similar to those of SY1207. The median grain sizes varied from 24 to 1240 μm in the survey area. Relatively large sizes were distributed north of the FDNPP (>37°25′N), whereas relatively small sizes occurred in the southern region (<37°25′N). Particularly, a band of very small grain sizes less than 100 μm were found around the southern region at depths of about 100 m. A similar horizontal pattern was also observed in the percentage of organic matter content (Fig. 6). Specifically, notably higher values up to almost 10% occurred in the southern region around the 100-m-depth region where the small grain sizes were found. Conversely, the contents were relatively low in the northern region where sediment grain sizes tended to be large.

4. Discussion

4.1. Horizontal distribution and difference of radiocesium between SY1202 and SY1207

Monitoring of radionuclides in the sea sediment was conducted extensively east of Japan by the Ministry of Education, Culture, Sports, Science and Technology (MEXT) until April 2013, and the Nuclear Regulation Authority (NRA) has conducted monitoring since that time. This monitoring includes the survey area of this study, and 19 of its locations overlapped those of the present study (see Fig. 2 in Kusakabe et al., 2013). The purpose of the present study was to reveal the detailed characteristics of the distribution of radiocesium concentration with enhanced spatial resolution by increasing the number of locations to 113. For example, the high-concentration band that was observed in the region south of the FDNPP was revealed to extend up to the area off the northern part of Ibaraki Prefecture with decreasing concentration. Although this feature was also indicated by Otosaka and Kobayashi (2013), who combined their survey data with the MEXT monitoring data, the present study further showed that the high-concentration band had an east–west width of about 20 km. Otosaka and Kobayashi (2013) also indicated the existence of a nearshore-to-offshore decreasing trend of radiocesium concentration from their observational data. However, the present study further ascertained that the monotonic decrease occurred to a depth of about 200 m, where the minimal concentration band existed, and that the concentrations increased once more beyond 200 m and then again decreased eastward.

Fig. 7 indicates the differences in the most-surface ^{137}Cs concentration (0–1 cm) at the overlapping survey stations off Fukushima Prefecture of SY1202 and SY1207. The decay rate of ^{137}Cs radioactivity is extremely small, about 1% during 5 months from February to July 2012. The range of the difference values was very

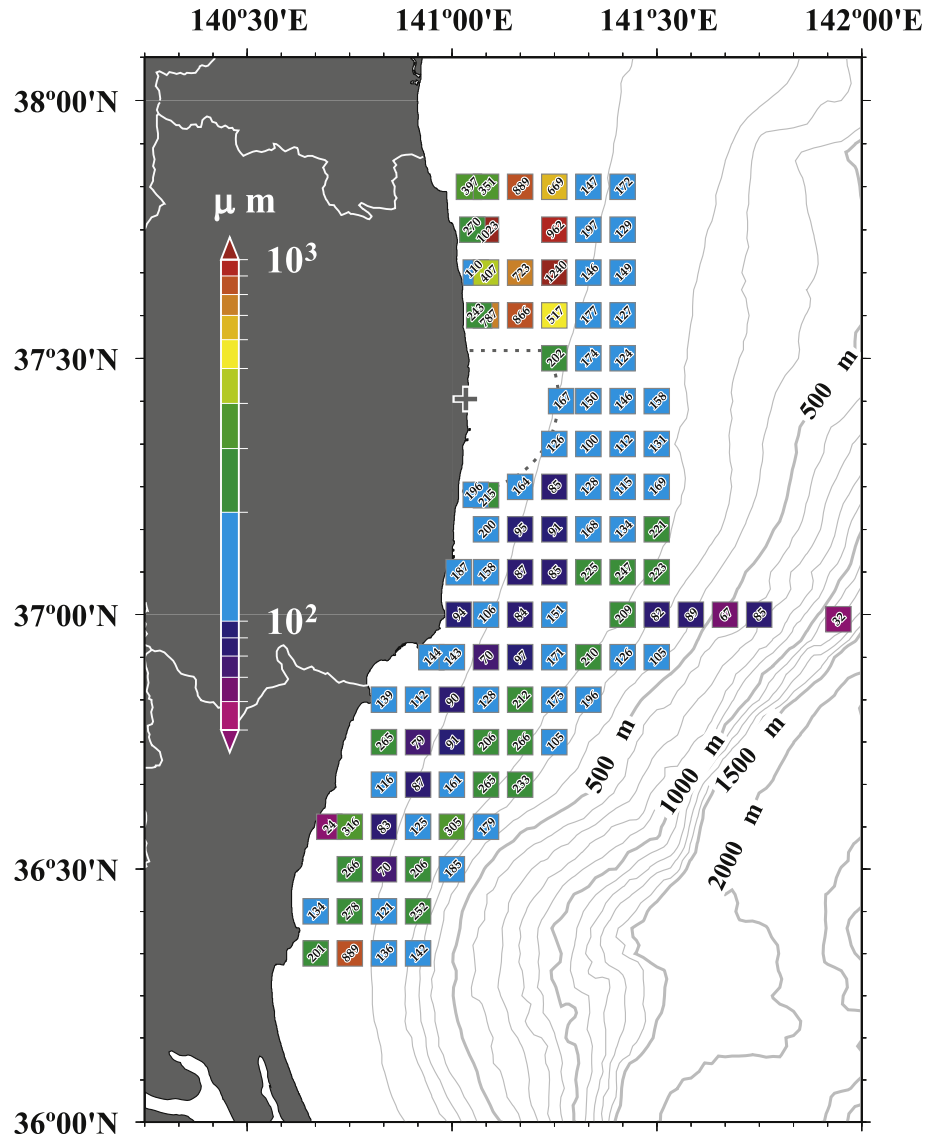

Fig. 5. Spatial distribution of median particle grain size (μm) of the most-surface (0–1 cm) sediment in July 2012. The color bar indicates grain size. The median grain sizes are also indicated within each tile. Contour lines indicate water depth at every 100 m. The cross and dotted circle indicate the location of the FDNPP and the border line of the caution zone, respectively.

large from −824 to 634 Bq/kg-dry, and the spatial average and standard deviation was −19 ± 197 Bq/kg-dry. However, although the difference values tended to be large around the 100-m isobaths, increasing/decreasing gaps between adjacent grids were often large and the spatial distribution of the difference values had a jagged pattern. One considerable reason for this result is variability of radiocesium concentration on spatial scale within a grid. For example, Kusakabe et al. (2013) conducted a multiple core sampling at a single location off Fukushima Prefecture. As a result, although the individual concentrations ranged within the same order, the standard deviation of the radiocesium concentrations had about half the magnitude of the mean value. Because the common grid points between SY1202 and SY1207 were not entirely at the identical location, because of local ship drifting etc., the radiocesium concentration values in the present study could also have variances with similar magnitude. Thus, it is difficult to quantitatively discuss the temporal change of the radiocesium concentrations in this study. However, the difference values did not exceed the order magnitude of the ^{137}Cs concentrations in SY1202 and SY1207, at each grid, suggesting that large spatial change of an order of several tens kilometers did not occur during the period from February to July 2012.

4.2. Mechanisms that determine horizontal distribution of radiocesium

The median grain size was large in the region north of the FDNPP where the radiocesium concentration was relatively low, and the band of small grain sizes was found around the 100-m isobaths in the southern region where the radiocesium concentration was very high (Figs. 3 and 6). This distribution of median grain size seemed to have already formed by at least 1996 as Aoyagi and Igarashi (1999) obtained a result very similar to this study. Fig. 8 shows scatter plots comparing median grain size and ^{137}Cs concentration of the most-surface samples in SY1202 and SY1207. Reasonably good correlations exist between the logarithmic values of the two parameters: correlation coefficients are −0.51 ($N = 40$, $p < 0.01$) and −0.38 ($N = 113$, $p < 0.01$) in SY1202 and SY1207,

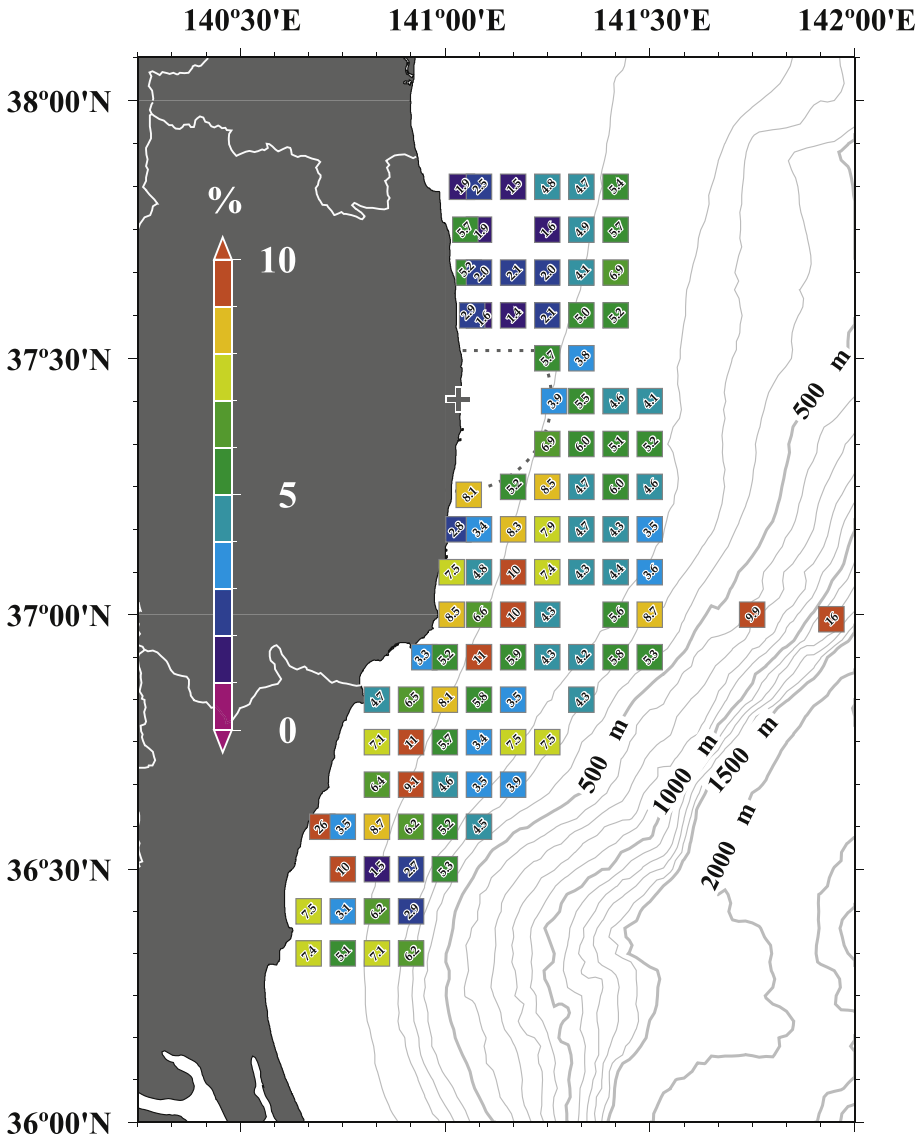

Fig. 6. Spatial distribution of the organic matter content (%) of the most-surface sediment in July 2012. The color bar indicates the ratio. The organic matter content values are also indicated within each tile. Contour lines indicate water depth at every 100 m. The cross and dotted circle indicate the location of the FDNPP and the border line of the caution zone, respectively.

respectively. We also obtained, in most cases by sieving the samples of SY1207, the similar result that the finer size fraction (<106 μm) of the sediment samples in this study had radiocesium concentrations similar with or several times higher than the concentration of the bulk sediment (data not shown). The grain-size related adsorption capability of sediment for cesium is suggested to be one of the factors that contributed largely to the formation of the spatial distribution pattern of radiocesium concentration. It is known that Cs has strong affinity with fine minerals, especially illite minerals (e.g., Børrentzen and Salbu, 2012; Comans et al., 1991; Comans and Hockley, 1992; Sakuma and Kawamura, 2011).

However, as a matter of course, other factors also can contribute to the determination of radiocesium concentration. In this study, the concentrations ranged over more than one order of magnitude in each similar grain size class. To consider the other factors, we divided the samples into five clusters by cluster analysis based on the group average method using logarithmic Euclidean distance on the coordinates of the median grain size and ^{137}Cs concentration (colors in Fig. 8b). Accordingly, we were able to detect three types of clusters by geographical dependence (Fig. 8c): (A) large grain sizes and low radiocesium concentrations which distributed at depths shallower than 100 m in the region north of the FDNPP (indicated with blue in Fig. 8b and c); (B) small grain sizes with high radiocesium concentrations which distributed mainly at depths shallower than 100 m, excepting the area of cluster (A) (indicated by red); and (C) small grain sizes with low radiocesium concentrations which were mainly in the area deeper than 100 m (indicated by yellow). The other two clusters were excluded from this discussion because their geographical features were unclear. The division of cluster (A) from the others can be attributed mainly to the low adsorption capability of large grain-size sediment for cesium, as mentioned above. One of the reasons for the division between clusters (B) and (C), which have a similar grain size range, could be the difference in the supply quantity of radiocesium to the sea bottom. For instance, monitoring of the radionuclides in seawater has been conducted at the same locations as sea sediment sampling (e.g., Oikawa et al., 2013) by MEXT and the NRA, and the radiocesium concentration data from September 2011 have been

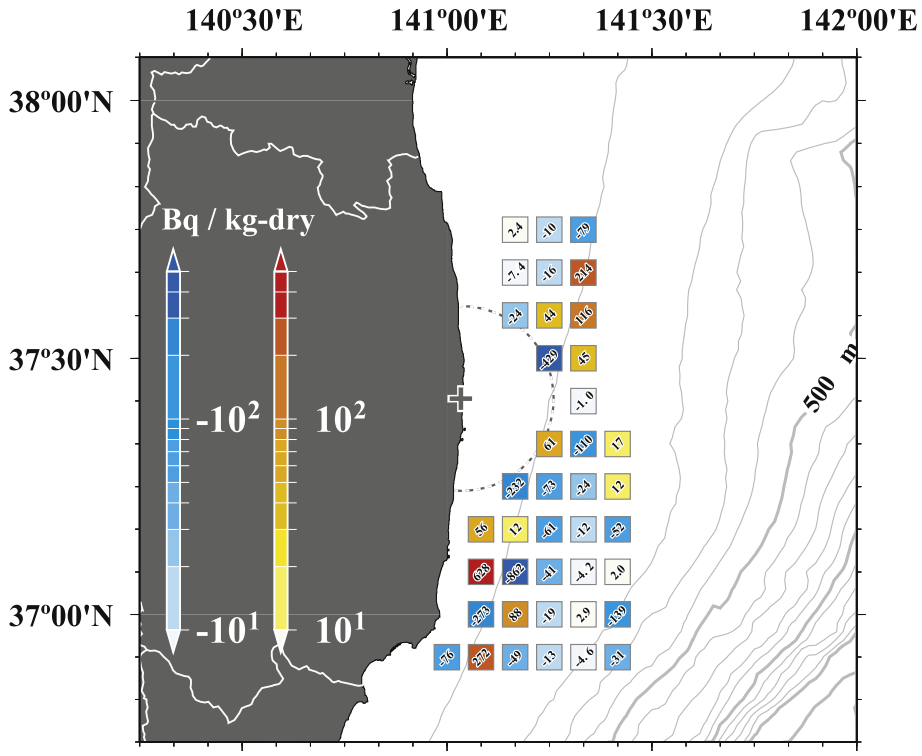

Fig. 7. Difference in ^{137}Cs concentrations in the most-surface sediment between February (Fig. 2g) and July (Fig. 3g). The cold and warm colors indicate a decrease and an increase from February to July, respectively. The difference values are also shown within each tile. Contour lines indicate the water depth at every 100 m. The cross and dotted circle indicate the location of the FDNPP and the border line of the caution zone, respectively.

published by website (NRA, 2014). Here, we used ^{137}Cs concentration data from the bottom layer (≤30 m above the seabed) from the northern Ibaraki to Fukushima Prefecture during the period of September 2011 to February 2012. These data were obtained by Ge detector measuring from coprecipitated and concentrated water samples with ammonium phosphomolybdate (for details, see Oikawa et al., 2013). Then, we divided these data into two groups: data from the area shallower than 100 m (C1, G0, I0, I1, and J1) and data from the area between 100 and 300 m (C3, G3, I3, and J2). The composite averages of the two groups of ^{137}Cs concentration data were 25.0 ± 18.1 mBq/L and 12.8 ± 9.5 mBq/L, respectively. This result potentially means that the average radiocesium supply capability in the shallower region was nearly twice as high as that in the deeper region even though the data used were expected to have been diffused horizontally because of the long elapsed time from 6 to 11 months after the FDNPP accident. Bailly du Bois et al. (2014) numerically simulated a transport of ^{137}Cs off Fukushima from March to June 2011 and showed that the ^{137}Cs concentration in the bottom layer could be more than one order higher in the area shallower than 100 m than that in the area deeper than 100 m during about two months after the FDNPP accident. Furthermore, a recent numerical study for demonstrating the formation process of the ^{137}Cs concentration distribution in sea sediment from March 2011 to March 2012 (Misumi et al., 2014) took into account the ^{137}Cs adsorption ability onto sediment from seawater and seemed to produce a spatial pattern of ^{137}Cs concentration similar to that in the present study since June 2011. Conversely, however, an indeterminate difference between ^{137}Cs concentration in the surface and bottom layer was also shown until at least two months after the accident by another numerical simulation for ^{137}Cs concentration in seawater from March to June 2011 (Rypina et al., 2013). Further research using numerical simulation for oceanic flow is needed to validate the radiocesium concentration in bottom seawater during the early period following the accident to estimate the proper difference in the radiocesium supply capability of those regions.

4.3. Vertical distribution of radiocesium

Although the vertical profiles of ^{137}Cs concentration decreased exponentially with depth in major cases, some locations had maximum concentration in a deeper layer instead of in the most-surface layer. To reveal the regional dependence of these vertical profile types, we converted the ^{137}Cs concentration values in each sediment layer of SY1202 and SY1207 to their relative proportion compared with the ^{137}Cs concentration in the most-surface layer at each location (Fig. 9). The ^{137}Cs concentrations in the lower layer sediments were similar to or at a higher level than those in the most-surface layer in the shallow area north of the FDNPP (e.g., Fig. 9k) where the larger grain sizes corresponding to cluster (A) in Fig. 8 distributed. The ^{137}Cs concentration magnitude of the most-surface sediment also tended to reach the lower layers along the coastal region. In other areas, the ^{137}Cs concentrations decreased in lower layers. For example, the ^{137}Cs concentration in the lowest layer was less than 10% of that of the most-surface layer around the 100-m isobaths.

The following three processes could possibly determine the characteristics of these vertical profiles. One is the desorption of radiocesium into pore water. This process requires that radiocesium in the sediment is not permanently adsorbed but rather exchangeably adsorbed to particles. The elution experiment from the sea sediment are required for validation of the process. Additionally, as the proportional relationship between sediment permeability and grain size is well known (e.g., Shepherd, 1989), dissolved radiocesium can migrate downward by a process similar to seawater diffusion in large-grain sediment. Therefore, percolation can be considered to occur greatly in the area of cluster (A) in

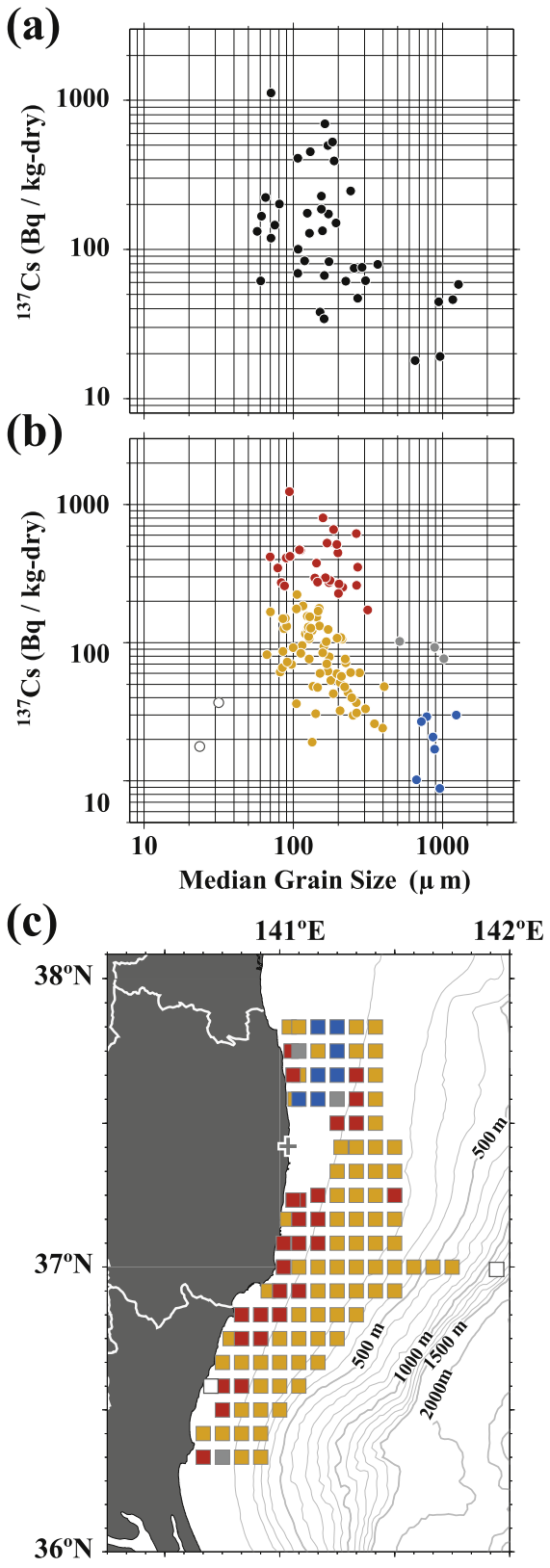

Fig. 8. Comparison between ^{137}Cs concentration and median grain size in the most-surface sediment obtained in February (a) and July (b) 2012. The color of the scatter in (b) shows the clusters segmented into five types by the group average method; the corresponding locations to these clusters are shown in (c).

Fig. 8. The second process is resuspension and redeposition by ocean waves or bottom flow. Because the radiocesium derived from the FDNPP is expected to initially deposit on the very surface of the seabed, resuspension that affects even a depth of several centimeters of sediment can easily mix or overturn contaminated and non-contaminated sediments. For example, Sato et al. (2000) reported that ocean waves can mix upper 40–80 cm sediment in interdecadal scale at the coastal area of southern part of Ibaraki Prefecture by the ^{210}Pb concentration in sediment cores. Furthermore, non-contaminated suspended particles can move the radiocesium concentration peak downward by being transported horizontally and redeposited on contaminated sediment at a different location. This process may be especially remarkable in the shallow region near by the coast where tidal effects are significant, as seen in Fig. 9. A recent report that estimated the mixing rate of sediment off Fukushima (Black and Buesseler, 2014) indicated that higher mixing occurred in the region shallower than 150 m. To investigate this process, at the least, a mooring system for measuring the bottom flow field is necessary. Thirdly, bioturbation could also be a possibility. Igarashi (1980) reported that non-selective deposit-feeder-type macro-benthos that burrow into sediment and ingest organic matter by eating the sediment often inhabited the area between the depth of 50 and 100 m off Fukushima. Black and Buesseler (2014) indicated that bioturbation could be intense in the shallow region. A culture experiment of the benthic animals in the sediment whose radiocesium concentration is given is also required for quantitative evaluation of this process. Thus, it is somewhat difficult to clarify the quantitative contributions of each process based on the data obtained in the present study. Further studies using multiple approaches based on physical, chemical, and biological analyses are needed to solve these problems.

4.4. Contribution of organic matter on the radiocesium distribution

Organic matter content was also found to have a similar spatial distribution pattern as that of ^{137}Cs concentration in SY1207. Specifically, organic matter content was correlated with ^{137}Cs concentration ($r = 0.38$, $p < 0.01$) as shown in Fig. 10. A significantly high correlation also existed between grain size and organic matter content ($r = -0.76$, $p < 0.01$: Fig. 11). In addition to minerals, organic matter can absorb radiocesium (Otosaka and Kobayashi, 2013). However, the lithogenic fraction contained most of ^{137}Cs in the sediment collected from the coastal area of Ibaraki, 70 km south of the FDNPP (Otosaka and Kobayashi, 2013). Accordingly, the grain size of sediment would directly link to the distributions of both the ^{137}Cs concentration and the organic matter content in sediment, although a quantitative evaluation of the contribution ratio between grain size and organic matter content to radiocesium concentration should remained an issue for future study in order to estimate the sea sediment impact on benthic marine ecosystems. Wada et al. (2013) reported that slow decreases of ^{137}Cs concentration were observed in demersal fishes in the southern region off of Fukushima and also that similar spatial distribution patterns of radiocesium concentration were observed between the demersal fishes and sediments. Based on this finding, they also hypothesized that the slow decrease in radiocesium concentration in the demersal fishes was caused by organic matter containing radiocesium in sea sediment and that the biologically available radiocesium (radiocesium in organic matter) would gradually translocate to the lithogenic fraction (radiocesium on minerals). Under this hypothesis, the radiocesium concentration of bulk sediment does not have temporal change at a position unless sediment moves. In addition to the radiocesium distribution of the present study being generally similar with their result, a high

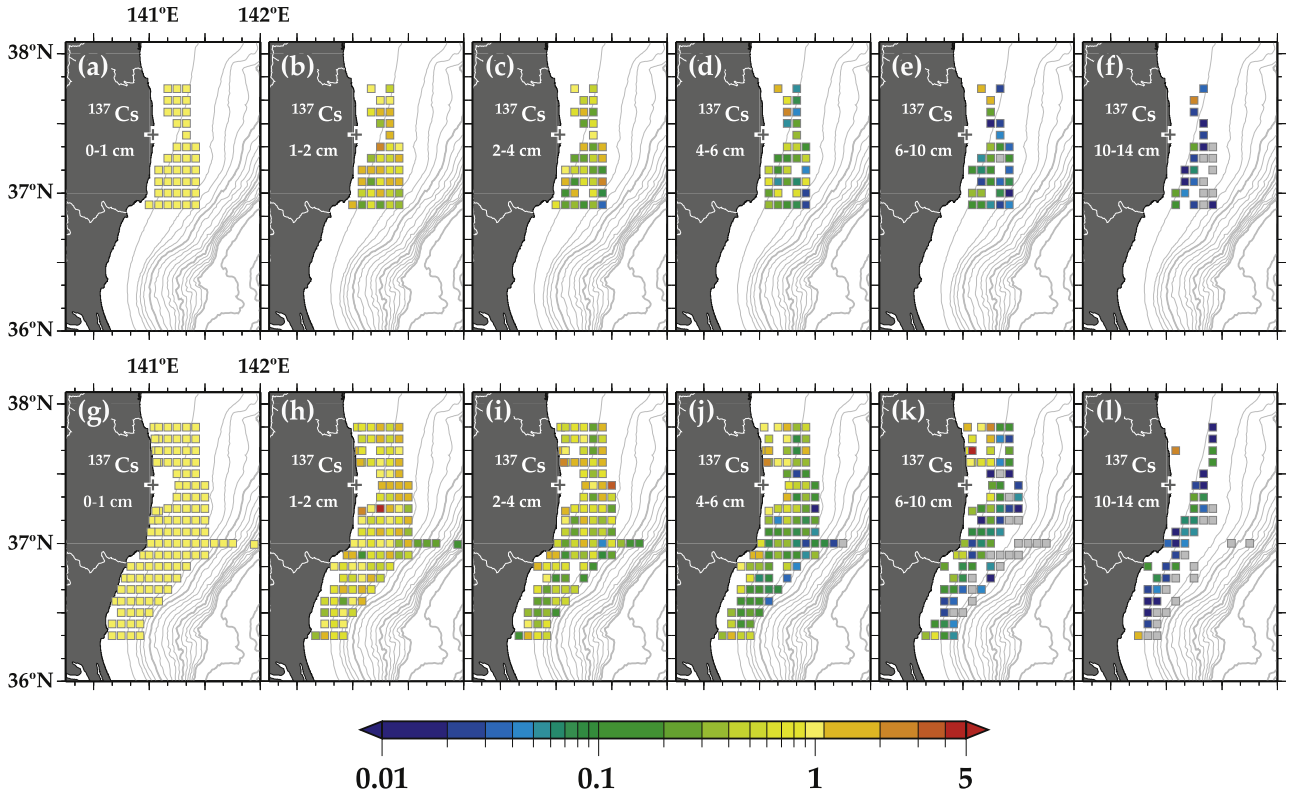

Fig. 9. Relative magnitude of ^{137}Cs concentration compared with the most-surface sediment at each location in February (a–f) and July (g–l) 2012. The respective layer is indicated at the side of each panel.

content of organic matter was also indicated in the southern region. Furthermore, the temporal change of the radiocesium distribution in the bulk sediment of this study was not significant, though the radiocesium in organic matter was unclear.

4.5. Distribution of radiocesium inventory

Assuming that the acquired radiocesium concentrations represent the values in each 5-min grid, we roughly estimated the ^{137}Cs inventory in SY1202 and SY1207 (Fig. 12a, b). Although density and water content for the each dried sediment sample are necessary to estimate the inventory, either one of those was missing in the present study due to the on-site sampling processes described in section 2. Therefore, to determine the ^{137}Cs inventory, we used bulk density and water content data by Kusakabe et al. (2013), which were obtained from identical sediment samples. Although their data were obtained from the upper 3 cm of the surface sediments,

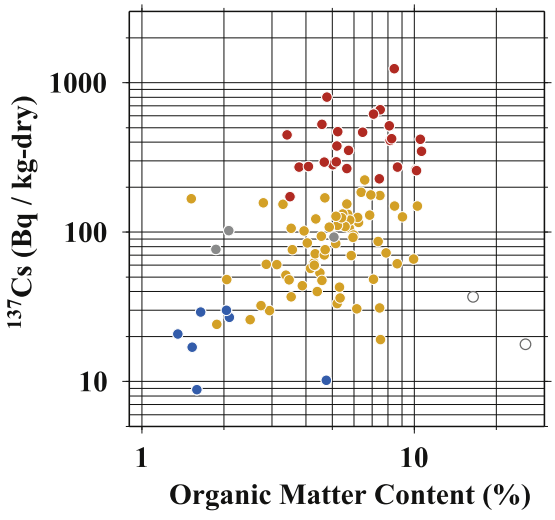

Fig. 10. Comparison between ^{137}Cs concentration and organic matter content ratio in the most-surface sediment in July 2012. The color of the scatter represents the segmented clusters corresponding to Fig. 8b.

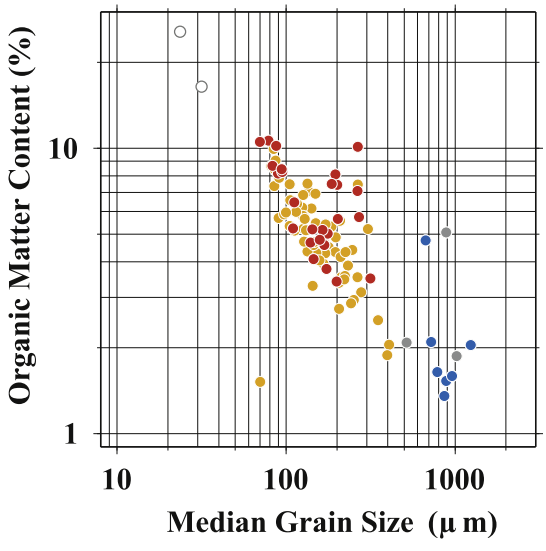

Fig. 11. Comparison between median grain size and organic matter content ratio in the most-surface sediment in July 2012. The color of scatter represents the segmented clusters corresponding to Fig. 8b.

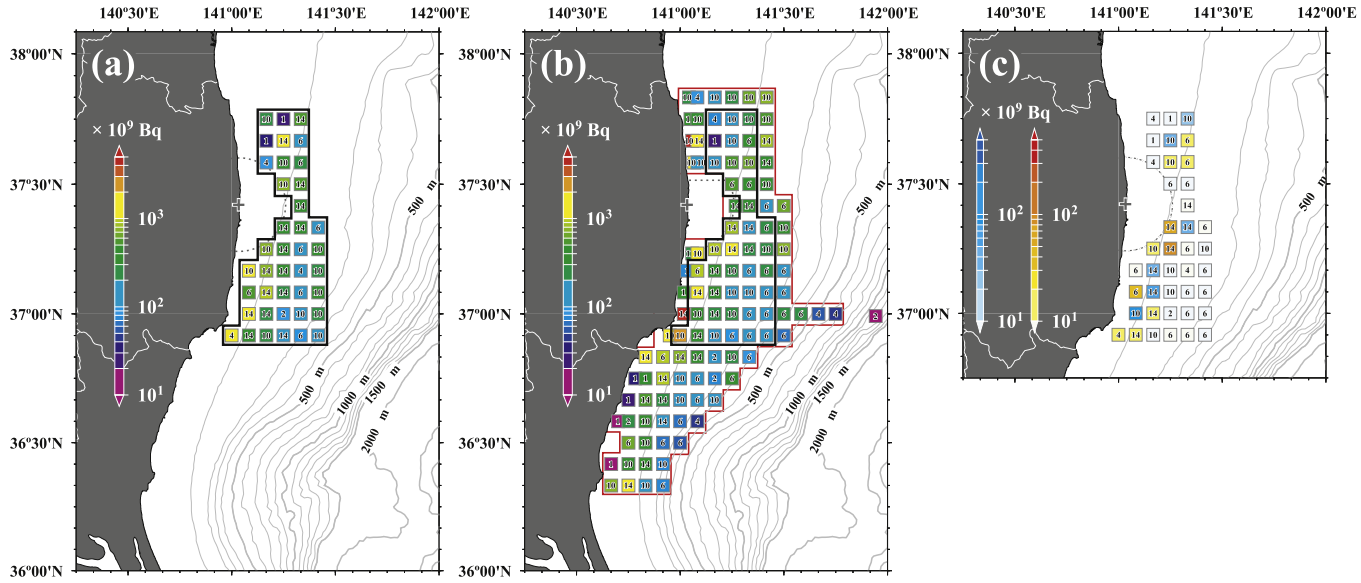

Fig. 12. Spatial distributions of ^{137}Cs inventories in the sediments in February (a) and July (b) 2012 and the-differences (c) derived by subtracting the values in February from those in July. At each location, the inventories of each layer were integrated from the most-surface sediment to the deepest collected layer depth (cm) (number on each tile). The total of the ^{137}Cs amounts in the sediments was estimated for the area enclosed by the black and red line in (a) and (b). (For interpretation of the references to color in this figure legend, the reader is referred to the web version of this article.)

we assumed that those data reflect properties of the sediment up to 14 cm. In addition, though the densities and water contents of their study were obtained during the period from May or September of 2011 to February 2012, the values did not seem to have changed much temporally. Therefore, we also assumed that these data did not change substantially after their study. First, the data were temporally averaged over the entirely of their period of investigation at each of their investigation locations. Then, the ^{137}Cs concentrations in SY1207 were converted to Bq/m^2 using the density and water-content averages from the nearest location.

The ^{137}Cs amounts from the most-surface to the 14-cm-depth in the common investigated area between SY1202 and SY1207 (the area for this estimation is shown by dotted black line in Fig. 12a, b) were respectively estimated at 1.98×10^{13} and 1.86×10^{13} Bq by vertically integrating the horizontal average inventories of each layer, meaning that the ^{137}Cs amount decreased by approximately 6% from February to July 2012 in this area. If this result is adequate, the amount of decrease can be expected to have been transported to other regions. However, the patterns of spatial increase and decrease were complex, and comprehensive movement of the ^{137}Cs was unclear from the difference distribution of the ^{137}Cs amounts between SY1202 and SY1207 (Fig. 12c). In this regard, more precise estimation is required in the future because of the unknown estimation error due to the local variability mentioned in section 4.1. The total amount of ^{137}Cs in the investigated area of SY1207 (the area for this estimation is shown with a red line in Fig. 12b), which was estimated by the same procedure, was 7.06×10^{13} Bq, or 1.96% of the total amount of ^{137}Cs released into the ocean (3.60×10^{15} Bq, reported by TEPCO, 2012).

5. Conclusions

In the present study, we constructed a 5-min gridded map of the radiocesium concentration in sea sediment from the region off the Fukushima Prefecture to the region off the northern part of Ibaraki Prefecture in February and July of 2012. The radiocesium released from the FDNPP was detected in the sediments at all survey locations. We revealed that the horizontal pattern of the radiocesium concentrations had a significant spatial scale of about 15–30 km in the east–west direction. The concentration values varied largely but were generally higher in the upper layers, and exceeded 2.00 kBq/kg-dry at the maximum in the most-surface sediment. Whereas high concentrations were often observed in the area south of the FDNPP, especially around the 100-m isobaths, a narrow band of minimal concentration was found along the 200-m isobaths. The horizontal pattern of the concentrations did not change clearly at spatial resolution of more than the 5-min grid scale during the period from February to July. In addition to a high correlation coefficient between the radiocesium concentration and grain size in the most-surface sediment, the geographical difference in the radiocesium amount in sea-bottom water was also suggested to correlate with the formation of the radiocesium distribution in the sediment. Moreover, these grain-size differences were suggested to affect the vertical profile of the radiocesium concentration partly.

Acknowledgments

We thank the captains and all the crew members of the R/V *Soyo Maru* for supporting the sample collection. We appreciate the great help from Mr. E. Okamoto of the Fisheries Research Agency (FRA), Japan, and Drs. S. Otosaka and T. Suzuki of the Japan Atomic Energy Agency (JAEA) who joined the sampling survey in SY1202 and SY1207, respectively. Mrs. M. Tanaka of FRA greatly supported the processing of the samples. This study was supported financially by the Fisheries Agency of Japan.

Appendix A. Supplementary data

Supplementary data associated with this article can be found in the online version, at http://dx.doi.org/10.1016/j.jenvrad.2014.09.007.

References

Aoyagi, K., Igarashi, S., 1999. On the size distribution of sediments in the coastal sea of Fukushima Prefecture. Bull. Fukushima Pref. Fish. Exp. Stat. 8, 69–81 (in Japanese).

Aoyama, M., Tsumune, D., Uematsu, M., Kondo, F., Hamajima, Y., 2012. Temporal variation of ^{134}Cs and ^{137}Cs activities in surface water at stations along the coastline near the Fukushima Dai-ichi Nuclear Power Plant accident site. Japan Geochem. J. 46 (4), 321–325.

Bailly du Bois, P., Garreau, P., Laguionie, P., Korsakissok, I., 2014. Comparison between modelling and measurement of marine dispersion, environmental half-time and ^{137}Cs inventories after the Fukushima Daiichi accident. Ocean Dyn. 64 (3), 361–383. http://dx.doi.org/10.1007/s10236-013-0682-5.

Black, E., Buesseler, K.O., 2014. Spatial variability and the fate of cesium in coastal sediments near Fukushima. Jpn. Biogeosci. Discuss. 11, 7235–7271. http://dx.doi.org/10.5194/bgd-11-7235-2014.

Børrentzen, P., Salbu, B., 2012. Fixation of Cs to marine sediments estimated by a stochastic modeling approach. J. Environ. Radioact. 61, 1–20.

Buesseler, K., Aoyama, M., Fukasawa, M., 2011. Impacts of the Fukushima Nuclear Power Plants on marine radioactivity. Environ. Sci. Technol. 45 (23), 9931–9935. http://dx.doi.org/10.1021/es202816c.

Comans, R.N.J., Hockley, D., 1992. Kinetics of cesium sorption on illite. Geochim. Cosmochim. Acta 56, 1157–1164.

Comans, R.N.J., Haller, M., DePreter, P., 1991. Sorption of cesium on illite: non-equilibrium behavior and reversibility. Geochim. Cosmochim. Acta 55, 433–440.

Honda, M.C., Kawakami, H., Watanabe, S., Saino, T., 2013. Concentration and vertical flux of Fukushima-derived radiocesium in sinking particles from two sites in the Northwestern Pacific Ocean. Biogeoscience 10, 3525–3534.

IAEA, 2004. Sediment Distribution Coefficients and Concentration Factors for Biota in the Marine Environment. IAEA, 95pp.

Igarashi, S., 1980. Characteristics of distribution of macro-benthos in the coastal region of Iwaki, Fukushima. Bull. Fukushima Pref. Fish. Exp. Stat. 6, 73–80 (in Japanese).

Kusakabe, M., Oikawa, S., Takata, H., Misonoo, J., 2013. Spatiotemporal distributions of Fukushima-derived radionuclides in nearby marine surface sediments. Biogeoscience 10, 5019–5030. http://dx.doi.org/10.5194/bg-10-5019-2013.

Masumoto, Y., Miyazawa, Y., Tsumune, D., Tsubono, T., Kobayashi, T., Kawamura, H., Estournel, C., Marsaleix, P., Lanerolle, L., Mehra, A., 2012. Oceanic dispersion simulations of ^{137}Cs released from the Fukushima Daiichi Nuclear Power Plant. Elements 8, 207–212. http://dx.doi.org/10.2113/gselements.8.3.207.

Misumi, K., Tsumune, D., Tsubono, T., Tateda, Y., Aoyama, M., Kobayashi, T., Hirose, K., 2014. Factors controlling the spatiotemporal variation of ^{137}Cs in seabed sediment off the Fukushima coast: implications from numerical simulations. J. Environ. Radioact. 136, 218–228.

NRA (Nuclear Regulation Authority), 2014. Monitoring information of environmental radio activity level (Readings of Seawater and Dust Monitoring in Sea Area by MEXT). http://radioactivity.nsr.go.jp/en/list/259/list-1.html.

Oikawa, S., Takata, H., Watabe, T., Misonoo, J., Kusakabe, M., 2013. Distribution of the Fukushima-derived radionuclides in seawater in the Pacific off the coast of Miyagi, Fukushima, and Ibaraki prefectures, Japan. Biogeoscience 10, 5031–5047. http://dx.doi.org/10.5194/bgd-10-4851-2013.

Otosaka, S., Kobayashi, T., 2013. Sedimentation and remobilization of radiocesium in the coastal area of Ibaraki, 70 km south of the Fukushima Dai-ichi Nuclear Power Plant. Environ. Monit. Assess. 185, 5419–5433. http://dx.doi.org/10.1007/s10661-012-2956-7.

Rypina, I.I., Jayne, S.R., Yoshida, S., Macdonald, A.M., Douglass, E., Buesseler, K., 2013. Short-term dispersal of Fukushima-derived radionuclides off Japan: modeling efforts and model-data intercomparison. Biogeoscience 10, 4973–4990. http://dx.doi.org/10.5194/bg-10-4973-2013.

Sakuma, H., Kawamura, K., 2011. Structure and dynamics of water on Li^+-, Na^+-, K^+-, Cs^+-, H_3O^+-exchanged muscovite surfaces: a molecular dynamics study. Geochim. Cosmochim. Acta 75, 63–81.

Sato, S., Maeda, R., Isobe, M., Sekimoto, T., Kasai, M., Yamamoto, K., 2000. Mechanism of sand drift in the Tone Estuary and condition of sediment supply to the coast of Hasaki. Proc. Coast. Eng. 47, 656–660 (in Japanese).

Shepherd, R.G., 1989. Correlations of permeability and grain size. Ground Water 27, 633–638. http://dx.doi.org/10.1111/j.1745-6584.1989.tb00476.x.

TEPCO (Tokyo Electric Power Co.), 2012. TEPCO News Press Releases. http://www.tepco.co.jp/en/press/corp-com/release/2012/1204659_1870.html.

Thornton, B., Ohnishi, S., Ura, T., Odano, N., Sasaki, S., Fujita, T., Watanabe, T., Nakata, K., Ono, T., Ambe, D., 2013. Distribution of local (137)Cs anomalies on the seafloor near the Fukushima Dai-ichi Nuclear Power Plant. Mar. Pollut. Bull. 74, 344–350. http://dx.doi.org/10.1016/j.marpolbul.2013.06.031.

Tsumune, D., Tsubono, T., Aoyama, M., Hirose, K., 2012. Distribution of oceanic ^{137}Cs from the Fukushima Dai-ichi Nuclear Power Plant simulated numerically by a regional ocean model. J. Environ. Radioact. 111, 100–108. http://dx.doi.org/10.1016/j.jenvrad.2011.10.007.

Wada, T., Kamiyama, K., Shimamura, S., Mizuno, T., Nemoto, Y., 2012. Effectiveness of stock enhancement of a rare species, spotted halibut *Verasper variegatus*, in Fukushima, Japan. Aquaculture 364–365, 230–239.

Wada, T., Nemoto, Y., Shimamura, S., Fujita, T., Mizuno, T., Sohtome, T., Kamiyama, K., Morita, T., Igarashi, S., 2013. Effects of the nuclear disaster on marine products in Fukushima. J. Environ. Radioact. 124, 246–254. http://dx.doi.org/10.1016/j.jenvrad.2013.05.008.